Chemical Geology 253 (2008) 38–49

Contents lists available at ScienceDirect

Chemical Geology

journal homepage: www.elsevier.com/locate/chemgeo

Controls on the metal compositions of magmatic sulfide deposits in the Emeishan large igneous province, SW China

Xie-Yan Song [a,b,*], Mei-Fu Zhou [a,b], Yan Tao [a], Jia-Fei Xiao [a]

[a] State Key Laboratory of Ore Deposit Geochemistry, Institute of Geochemistry, Chinese Academy of Sciences, Guiyang, 550002, PR China
[b] Department of Earth Sciences, The University of Hong Kong, Hong Kong, PR China

ARTICLE INFO

Article history:
Received 16 September 2007
Received in revised form 20 February 2008
Accepted 5 April 2008

Editor: D. Rickard

Keywords:
Magmatic sulfide deposit
Emeishan large igneous province
Multiple removal of sulfide liquid
R-factors

ABSTRACT

Magmatic sulfide deposits in the Emeishan large igneous province, SW China, have variable chalcophile and siderophile metal contents and can be divided into PGE, Ni–Cu–PGE and Ni–Cu deposits. PGE sulfide deposits include the Jinbaoshan and Zhubu deposits and have ores with very low sulfide contents (~1 to 2 vol.%) and very high Pt and Pd (0.3 to 10 ppm) and Ir (0.02 to 0.5 ppm). Typical Ni–Cu–PGE sulfide deposits include the Yangliuping and Qingkuangshan deposits, which contain sulfide ores with more than 10 vol.% sulfides (0.1–6.2 wt.% Ni, 0.03–11 wt.% Cu) and have moderate PGE contents (0.1–5 ppm Pt, 0.01–1.8 ppm Pd, <0.5 ppm Ir). The Ni–Cu sulfide deposits, such as the Limahe and Baimazhai deposits, have sulfide-rich ores with more than 10 vol.% sulfides (0.1–4 wt.% Ni, 0.02–6.5 wt.% Cu) and are extremely poor in PGE (<0.2 ppm Pt and <0.3 ppm Pd, <0.007 ppm Ir). Silicate rocks from the hosting intrusions of these three types of deposits have distinctive PGE concentrations.

On the 100% sulfide basis, Pt and Pd correlate positively with Ir in the ores from the PGE deposits, whereas they correlate negatively in the Ni–Cu–PGE and Ni–Cu deposits. PGE geochemistry and model calculations indicate that the PGE-rich sulfides were separated from primary basaltic magmas, whereas the Ni–Cu–PGE sulfides were produced from magmas that had experienced minor sulfide removal (about 0.01%), and the Ni–Cu sulfides were separated from magmas that experienced about 0.025% sulfide segregation. Fractionation of monosulfide solid solution resulted in differentiation between IPGE and PPGE in the Ni–Cu–PGE and Ni–Cu deposits.

1. Introduction

Magmatic sulfide deposits may be sulfide-rich or sulfide-poor and contain variable contents of Ni, Cu and platinum group elements (PGE). Some sulfide-rich deposits, such as the Noril'sk-Talnakh deposit, Russia (Naldrett et al., 1995), are rich in base metals and PGE, whereas others, such as the Voisey's Bay deposit, Canada (Naldrett et al., 2000) and the Jinchuan deposit, NW China (Chai and Naldrett, 1992; Song et al., 2006) are PGE-poor. Sulfide-rich deposits often occur in dynamic magmatic systems such as lava channels and magma conduits, whereas sulfide-poor and PGE-rich deposits generally occur in large layered intrusions (Li et al., 2001). There is general agreement that PGE contents in sulfide ores are strongly dependent on metal compositions in the parental silicate magmas and the ratios between sulfide liquid and silicate magma (defined as *R*-factor) (Campbell and Naldrett, 1979). However, PGE abundances and *R*-factors may vary for each pulse of parental magma involved in the magmatic system. In addition, contents of Ni, Cu, and PGE in the sulfide ores may be affected by differentiation of the sulfide melt. The key factors controlling variable Ni, Cu and PGE contents of magmatic sulfide deposits are not completely understood and need to be re-evaluated.

There are many magmatic sulfide deposits and sulfide-bearing intrusions in the Emeishan large igneous province (ELIP), SW China (Zhou et al., 2002a, 2005; Song et al., 2005). The ELIP, which was produced by a mantle plume at ~260 Ma, is divided into a central and outer zone (Fig. 1) (Xu et al., 2004; Song et al., 2005). The central zone is characterized by a thick sequence of continental flood basalts and large layered mafic and syenitic intrusions (e.g. Zhang and Luo, 1988). In contrast, the outer zone has a relatively thin flood basalt sequence (less than 1000 m) and small mafic–ultramafic intrusions. Giant magmatic oxide deposits, including Panzhihua, Hongge, and Baima, are hosted in layered intrusions in the central zone (Zhou et al., 2005), whereas magmatic sulfide deposits, including Yangliuping, Baimazhai, Jinbaoshan, Limahe, and Qingkuangshan, occur in both the central and outer zones (Fig. 1) (Zhang and Luo, 1988; Zhou et al., 2002a; Song et al., 2005). Recent studies have shown that these sulfide deposits have variable metal concentrations (Song et al., 2003, 2004; Wang and Zhou, 2006; Tao et al., 2007). Song et al. (2003) proposed that the Yangliuping sulfide deposit was formed by concentration of sulfide

* Corresponding author. State Key Laboratory of Ore Deposit Geochemistry, Institute of Geochemistry, Chinese Academy of Sciences, 64th Guanshui Road, Guiyang, 550002, PR China. Tel./fax: +86 851 5895538.
E-mail address: songxieyan@vip.gyig.ac.cn (X.-Y. Song).

0009-2541/$ – see front matter © 2008 Elsevier B.V. All rights reserved.
doi:10.1016/j.chemgeo.2008.04.005

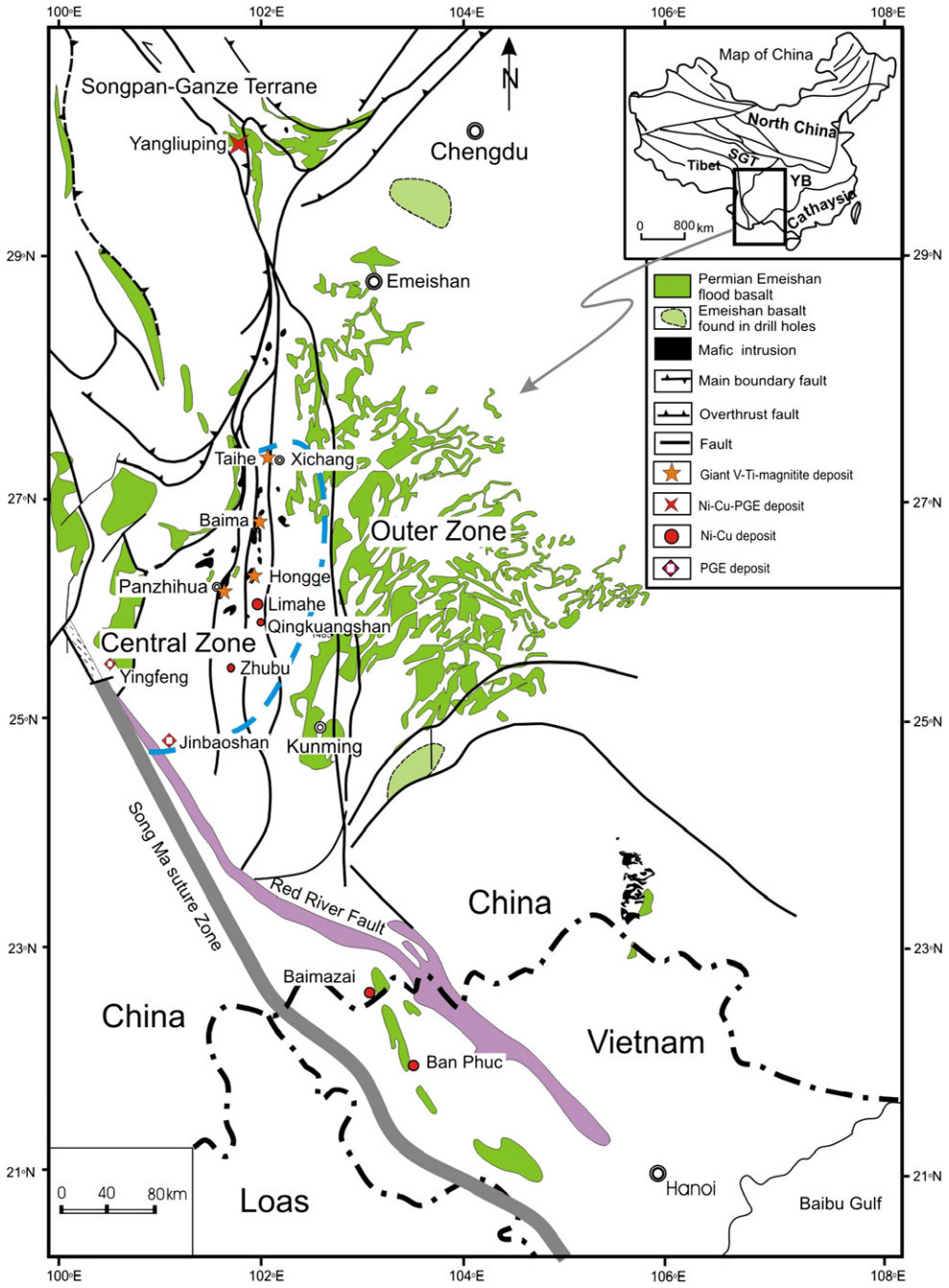

Fig. 1. Simplified geological map of the Emeishan large igneous province, showing outcrops of the Emeishan flood basalts and locations of main magmatic sulfide deposits and giant V–Ti magnetite deposits. YZ: Yangtze Block; SGT: Songpan-Ganzi Terrane.

melts at the base of sill-like magma chambers and that sulfide immiscibility was triggered by assimilation fractional crystallization (AFC) processes and the introduction of S and CO_2 from the wall rocks. Only limited PGE data are available for this deposit (Song et al., 2003). The Jinbaoshan sulfide deposit is marked by high PGE grades and was thought to have been formed by accumulation of immiscible sulfide droplets from magmas in a sill-like conduit where they reacted with new magmas passing through the conduit (Tao et al., 2007). The extremely low PGE concentrations in the Baimazhai deposit were interpreted to have resulted from very low *R*-factor (=70) (Wang and Zhou, 2006). However, the key factors controlling the different PGE concentrations in these deposits, such as multiple sulfide segregation and fractionation of sulfide liquid have not been investigated. In addition, PGE concentrations of the hosting silicate rocks should contain information about the origin of magmatic sulfides, because the hosting intrusions and associated sulfide ores were usually produced from the same magma systems.

In this paper, we present new data on chalcophile and siderophile elements for 24 sulfide ores and 15 silicate rocks from the Yangliuping, Limahe and Qingkuangshan deposits in the ELIP. We also utilize published data for both sulfide ores and silicate rocks from the Baimazhai and Jinbaoshan deposits (Wang and Zhou, 2006; Tao et al., 2007) in order to examine the roles of PGE abundances of parental basaltic magmas, multiple sulfide segregation, and fractionation of sulfide melts in controlling the metal contents of the ELIP deposits. The use of PGE abundances in the host silicate rocks for exploration of different types of sulfide mineralization is also evaluated.

2. Geological background

Southwest China comprises the Yangtze Block in the east and the Tibetan Plateau in the west (Fig. 1). The easternmost part of the Tibetan Plateau is represented by the Songpan-Ganze Terrane, which is characterized by thick (up to 10 km or more) Triassic marine clastic strata (Burchfiel et al., 1995). The Yangtze Block contains a Proterozoic metamorphic basement overlain successively by Paleozoic marine sedimentary strata, and Triassic or younger terrestrial basin deposits.

The ELIP crops out over an area of more than 5×10^5 km^2 in the western part of the Yangtze Block and the eastern margin of the Tibetan Plateau, and extends from SW China into northern Vietnam. It comprises the Emeishan continental flood basalts and associated mafic–ultramafic intrusions and is considered to have formed from a Permian mantle plume (Chung and Jahn, 1995; Xu et al., 2001; Song et al., 2001; Zhou et al., 2002b). The ELIP is divided into a central and outer zone (Xu et al., 2004; Song et al., 2005) (Fig. 1), and the flood basalts range from more than 2000 m thick in the central zone to several hundred meters thick in the outer zone (Xu et al., 2004; Song et al., 2005). The volcanic sequence consists primarily of tholeiitic basalt with minor picrite, basaltic andesite, and tephrite.

Several giant V–Ti–Fe oxide deposits are hosted in large layered intrusions, such as the Baima, Panzhihua and Hongge deposits in the central zone (e.g. Zhang and Luo, 1988; Zhou et al., 2002a; Zhong et al., 2002, 2003, 2004; Zhou et al., 2005). In contrast, magmatic sulfide deposits occur widely in both the central and outer zones. The most important of these are the Jinbaoshan, Limahe, and Qingkuangshan deposits in the central zone and the Yangliuping, Baimazhai and Ban Phuc deposits in the outer zone (Fig. 1) (Glotov et al., 2001; Song et al., 2003, 2004, 2005; Wang and Zhou, 2006). Some mafic–ultramafic

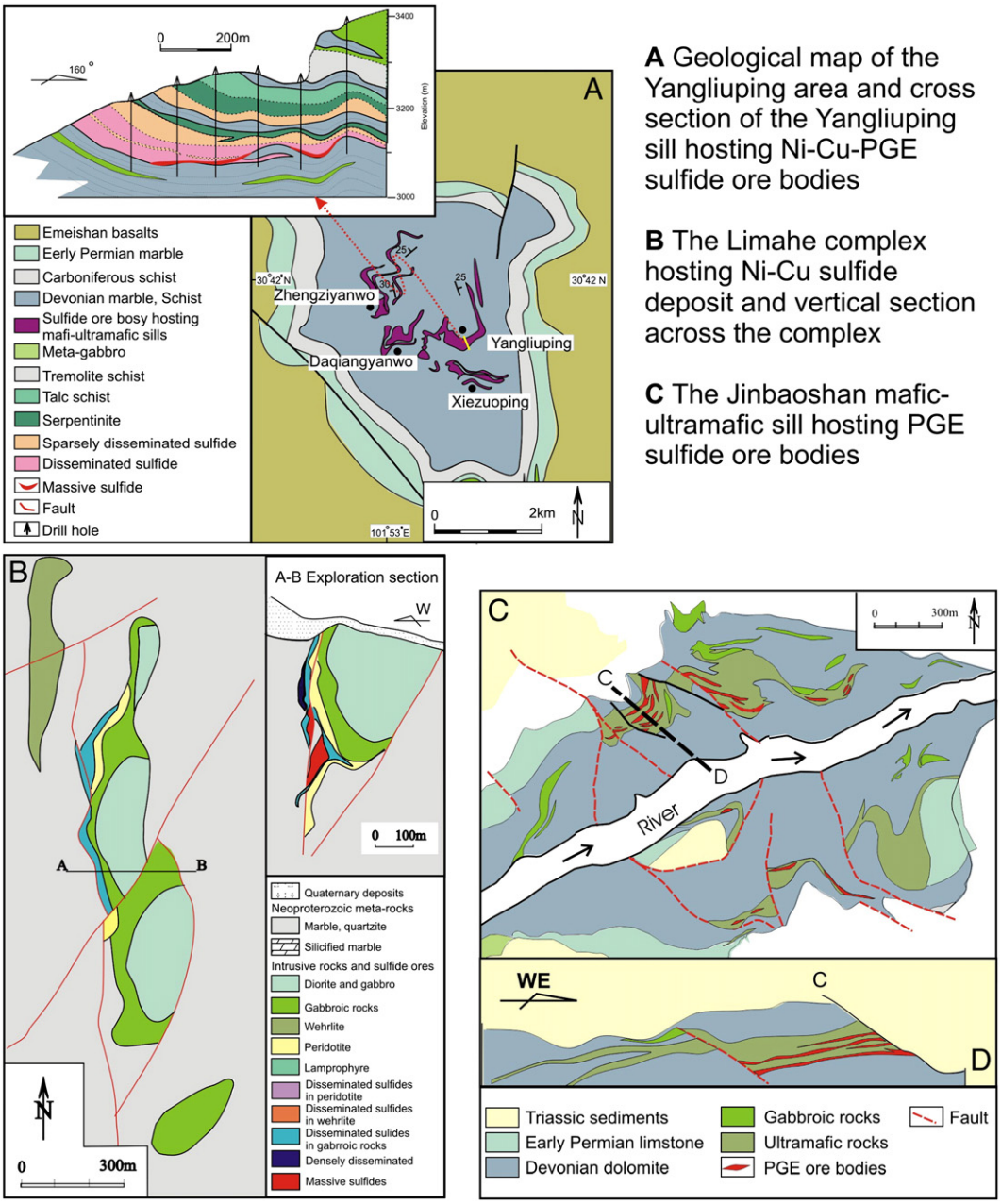

Fig. 2. Geological maps of typical magmatic deposits in the ELIP. (A) Geological map of the Yangliuping area showing distribution of the intrusions hosting sulfide deposits and a vertical section of the Yangliuping sill; (B) Geological map of the Limahe intrusion and a vertical section of the intrusion; (C) Geological map of the Jinbaoshan ultramafic sill and a cross section showing distribution of the PGE sulfide layers.

intrusions in the central zone also have uneconomic Ni–Cu–(PGE) sulfide mineralization (Yao, 1988). The host mafic–ultramafic intrusions occur as sills, dikes, or small bodies intruding the Proterozoic metamorphic rocks and Paleozoic sedimentary rocks.

3. Magmatic sulfide deposits

The majority of magmatic sulfide deposits in the ELIP, such as the Yangliuping, Limahe, Qingkuangshan, Baimazhai, and Ban Phuc deposits (Glotov et al., 2001; Song et al., 2003, 2004; Wang and Zhou, 2006), are sulfide-rich with more than 10 vol.% sulfides. A few deposits, such as the Jinbaoshan, Yingfeng, and Zhubu are sulfide-poor with less than 3 vol.% sulfides in the ores (Song et al., 2005; Tao et al., 2007) (Fig. 1).

3.1. Sulfide-rich deposit

The sulfide-rich deposits, including the Yangliuping and Baimazhai deposits, have recently been studied by Song et al. (2003, 2004) and Wang and Zhou (2006). In the Yangliuping area, at the northernmost margin of the ELIP, there are four sulfide-bearing mafic–ultramafic sills, the Yangliuping, Zhengziyanwuo, Xiezuoping, and Daqiangyanwo bodies, hosted in Devonian quartz schist and marble within a tectonic dome (Song et al., 2003, 2004) (Figs. 1 and 2A). Economic sulfide orebodies occur in the Yangliuping and Zhengziyanwuo sills. These sills are 2–3 km long, up to 300 m thick, and extend 300–500 m along the dip. They consist, from the base upward, of serpentinite, talc schist, tremolite schist, and metagabbro (Song et al., 2003). More than 90% of the Ni, Cu, and PGE reserves are contained in stratiform orebodies (generally 10–50 m but up to 90 m thick) mainly within the serpentinite at the base of the sills. The amounts of sulfide decrease regularly from >30 vol.% in the lower zone to <20 vol.% in the upper zone of the orebodies. Weakly mineralized zones, with <10 vol.% sulfide occur above the stratiform orebodies. The massive ores occur at the bottom of the disseminated orebody and/or extend to the footwall marble. The mineral assemblage is pyrrhotite + chalcopyrite + pentlandite. Platinum group minerals, including sperrylite, testibiopalladite, and Pd-bearing melonite, have been identified in the sulfides (Song et al., 2004). The Yangliuping and Zhengziyanwuo deposits are simply termed the Yangliuping deposit in the following sections.

The Baimazhai deposit at the southern margin of the ELIP (Figs. 1 and 2B) is hosted in a lens-shaped mafic–ultramafic body, ~530 m long, ~190 m wide and 24 to 64 m thick that intrudes Ordovician meta-sandstone and slate (Wang and Zhou, 2006). The mafic–ultramafic intrusion is a concentric body composed of an inner core of massive sulfide ores surrounded by orthopyroxenite, websterite and gabbro. The orthopyroxenite and websterite contain net-textured and disseminated sulfides, respectively, whereas the gabbro is poor in sulfide. The dominant sulfide minerals in the ores are pyrrhotite, chalcopyrite, and pentlandite (Wang and Zhou, 2006).

The Limahe deposit in the central zone of the ELIP is hosted in a lopolith-like mafic–ultramafic intrusion (Fig. 1). The intrusion is 900 m long and 20–180 m wide, dips 70–90° to the west and extends to a depth of 800 m (Fig. 2B). It is hosted in Proterozoic metamorphic rocks. The intrusion consists of gabbro and diorite, and peridotite occurs along the western margin and base of the intrusion. The boundaries between the peridotite and the gabbro are sharp. The zircon U–Pb isotope age of the Limahe intrusion is 262±2 Ma (Zhou, 2004). The peridotite is strongly mineralized with disseminated and net-textured sulfides. The main disseminated sulfide orebody is 500 m long and 2 to 29 m thick. An irregularly-shaped massive orebody is emplaced along the margin of the disseminated orebody and shows an intrusive contact with both the disseminated orebody and the metamorphic wall rocks of the intrusion.

The Qingkuangshan ultramafic dike is located at the central zone of the ELIP and hosts a sulfide-rich orebody (Fig. 1). The north–south trending dike is only about 200 m long and less than 80 m wide and intruded Proterozoic schists. Peridotite occurs in the middle part of the dike and is surrounded by gabbro to the north. The dike becomes narrow downward and the gabbro disappears gradually at a depth of ~100 m. The peridotite is almost totally mineralized with disseminated and net-textured sulfides. The sulfides are concentrated in the central part of the peridotite.

3.2. Sulfide-poor deposits

The Jinbaoshan, Yingfeng, and Zhubu deposits in the central zone are sulfide-poor but PGE-rich (Fig. 1). The Jinbaoshan deposit is the largest Pt–Pd sulfide deposit in China and is hosted in a mafic–ultramafic sill, 5000 m long, 600–1000 m wide, and <170 m thick (Fig. 2C). The Jinbaoshan sill intrudes Devonian dolomite and comprises mainly wehrlite and peridotite, with gabbro in its upper part (Brozdowski Page, 2004; Tao et al., 2007). Economic Pt–Pd sulfide ores are mainly hosted in wehrlite as two sub-horizontal layers with thicknesses of 4–16 m in the basal and middle parts of the sill. The Pt–Pd rich layers are characterized by 1–3 vol.% sulfides and 9–20% chromite. The sulfide mineral assemblage includes pyrrhotite, chalcopyrite, and pentlandite. Platinum group minerals in the sulfides are mainly sperrylite, testibiopalladite and niggliite (Yang, 1989). Previous exploration suggests reserves of 9.44 million tones of ore with average PGE grades of 0.9–1.66 ppm.

4. Analytical methods

Whole-rock S contents for the sulfide ores and silicate rocks were determined using a gravimetric method and IR-absorption spectrometry, respectively in the Institute of Geochemistry in Guiyang, China. The detection limits of IR-absorption spectrometry are about 1 μg/g and the accuracies are estimated to be better than ±8%. Nickel and Cu of the samples were determined using the Philips PW 2400 X-Ray Fluorescence Spectrometer in the Department of Earth Sciences of The University of Hong Kong and by a gravimetric method in the Institute of Geochemistry of Chinese Academy of Sciences. The technique of NiS fire assay coupled with Te co-precipitation (Qi et al., 2004) was used for PGE analyses in the Chinese Academy of Geological Sciences and Department of Earth Sciences in The University of Hong Kong. The precision and accuracy as demonstrated by analyzing reference materials, UMT-1 and WPR-1, are better than 10%. The procedural blanks were generally less than 1 ppb: Ir <0.15 ppb, Ru <0.15 ppb, Rh <0.05 ppb, Pt <0.5 ppb, Pd <0.5 ppb.

5. Analytical results

5.1. Classification of the sulfide deposits on the basis of metal contents

As described above, the magmatic sulfide deposits in the ELIP include sulfide-poor and sulfide-rich deposits. Sulfide-rich deposits can be further divided into Ni–Cu and Ni–Cu–PGE deposits.

The Jinbaoshan, Yingfeng, and Zhubu deposits are sulfide-poor, and PGE-rich, and are referred to as PGE deposits. The Jinbaoshan PGE deposit contains sparsely disseminated sulfide ores with very low S contents (up to 1.8 wt.%) and low Ni and Cu contents (<0.2% and <0.3%, respectively) and are characterized by extremely high Pt (350–10,240 ppb), Pd (190–6430 ppb) and Ir (up to 500 ppb) relative to ores with similar S contents in the sulfide-rich deposits (Table 1, Fig. 3A–E) (Tao et al., 2007).

Both Ni–Cu and Ni–Cu–PGE deposits have similar Ni, Cu, and S contents, although some massive sulfide ores in the Yangliuping and Baimazhai deposits are relatively poor in Cu (Table 1, Fig. 3A, B), and display two separate trends in the plots of PGE against S (Fig. 3C–E). The Ni–Cu–PGE deposits, such as the Yangliuping and Qingkuangshan bodies, are rich in Ni, Cu and PGE. However, the Ni–Cu deposits,

Table 1
Concentrations of Ni, Cu, and PGE of the sulfide ores of the important magmatic sulfide deposits and host rocks in the Emeishan large igneous province

	Ni–Cu sulfide deposits									
Intrusion	Limahe									
Rock/ore	Websterite				Gabbro				Disseminated ore	
Sample	SL05-7	SL05-8	SL05-9	SL05-10	SL05-1	SL05-2	SL05-3	SL05-5	SL05-11	SL05-13
Ni (ppm)	822	1116	834	591	265	157	268	1012	1619	13,743
Cu (ppm)	98	201	151	75	180	110	132	265	427	8125
S (ppm)	2700	2000	2100	3400	1900	1100	500	2500	122,900	33,901
Ir (ppb)	0.20	0.08	0.08	0.05	0.19	0.07	0.03	0.07	0.65	3.75
Ru (ppb)	0.54	0.85	1.09	0.57	0.73	0.72	0.39	0.53	1.70	9.07
Rh (ppb)	0.08	<0.02	<0.02	<0.02	0.13	0.05	0.02	0.06	0.17	1.50
Pt (ppb)	0.84	0.70	0.47	0.56	3.10	1.77	0.43	2.38	2.50	14.1
Pd (ppb)	1.73	0.43	0.55	0.33	3.95	2.23	0.43	3.10	3.32	4.61

	Ni–Cu–PGE sulfide deposit									
Intrusion	Yangliuping sill									
Rock/ore	Serpentinite	Talc	Tremolite	Massive ore				Net-textured ore		
Sample	Y01-21	Y01-15	Y01-5	Y01-44	Y01-57	Y02-2	Y02-3	Y01-38	Y01-53	Y01-49
Ni (ppm)	1543	1378	573	55,744	55,309	39,362	45,415	4351	1626	9041
Cu (ppm)	66	179	102	4495	370	112,913	99,967	14,621	4408	12,423
S (ppm)	936	1562	773	299,600	343,300	337,100	337,400	26,600	17,300	75,300
Ir (ppb)	1.78	2.54	0.99	191.5	483.4	212.7	162.1	1.1	2.15	1.61
Ru (ppb)	6.34	7.10	2.66	409.7	674.0	445.0	518.8	2.9	11.62	25.19
Rh (ppb)	0.58	1.24	0.56	239	332	292	225	20.3	9.5	26.1
Pt (ppb)	10.95	46.49	12.83	1308	1126	2236	4867	1734	138	359
Pd (ppb)	13.30	30.95	11.13	1797	380	886	1786	288	79	26

	Ni–Cu–PGE sulfide deposit									
Intrusion	Yangliuping sill		Zhengziyanwuo sill							
Rock/ore	Disseminated ore		Serpentinite	Talc		Gabbro	Massive ore			Net-textured ore
Sample	Y01-55	YD-2	Z01-8	Z01-11	Z01-13	Z01-20	Z01-1	ZD-22	ZD-25	Z01-37
Ni (ppm)	15,813	21,949	1754	1438	491	144	50,193	61,651	61,924	18,408
Cu (ppm)	60,322	6163	416	161	119	57	1284	293	261	3754
S (ppm)	166,200	113,600	2122	1282	344	319	260,500	347,300	347,500	102,000
Ir (ppb)	26.7	16.6	1.13	1.58	0.56	0.17	521.4	106.4	62.0	17.1
Ru (ppb)	76.5	44.0	5.35	5.86	0.75	0.20	1033.0	117.1	88.3	30.5
Rh (ppb)	42.9	41.3	0.65	0.67	0.41	0.12	339	148	141	58.7
Pt (ppb)	1378	3819	157.59	25.14	9.47	6.70	1247	1997	1493	675
Pd (ppb)	667	1135	82.07	20.64	18.10	4.25	150	487	682	263

	Ni–Cu sulfide deposits								
Intrusion	Zhengziyanwuo sill						Qingkuangshan		
Rock/ore	Net-textured ore			Disseminated ore			Disseminated ore		
Sample	Z01-40	Z01-43	Z02-1	Z02-2	Z01-6	Z01-32	SQ05-4	SQ05-8	SQ05-9
Ni (ppm)	10,390	5677	25,184	6531	3886	6827	6504	5749	1262
Cu (ppm)	9183	50,255	35,844	10,746	1416	2260	8889	11,352	3927
S (ppm)	68,600	85,800	144,200	50,700	25,400	33,100	38,800	40,100	9300
Ir (ppb)	24.6	7.2	60.0	31.9	1.3	2.8	10.7	7.72	1.35
Ru (ppb)	82.1	16.0	94.5	99.0	3.6	14.6	4.78	2.65	1.29
Rh (ppb)	38.2	45.7	86.8	38.7	3.8	10.0	6.73	5.43	0.90
Pt (ppb)	704	2449	1654	665	494	410	311	387	164
Pd (ppb)	132	146	855	272	167	280	593	861	351

Many data used in the figures in this paper, including some data of the Limahe Ni–Cu sulfide deposit (from Tao et al., submitted for publication), data of the Jinbaoshan Pt–Pd sulfide deposit (from Tao et al., 2007), and data of the Baimazhai Ni–Cu sulfide deposit (from Wang and Zhou, 2006) are not listed in this table.

such as the Limahe and Baimazhai deposits, are extremely poor in PGE, (Table 1). The sulfide ores of the Yangliuping and Qingkuangshan Ni–Cu–PGE deposits contain 150–1797 ppb Pt, 350–4867 ppb Pd, 1–521 ppb Ir, 4–1033 ppb Ru, and 4–339 ppb Rh, whereas those of the Limahe and Baimazhai Ni–Cu deposits have <313 ppb Pd, <222 ppb Pt, <7 ppb Ir, <120 ppb Ru, and <12 ppb Rh (Table 1, Wang and Zhou 2006).

In summary, the magmatic sulfide deposits in the ELIP can be divided into three types: Ni–Cu–PGE sulfide deposits (Yangliuping and Qingkuangshan), Ni–Cu sulfide deposits (Limahe and Baimazhai) and PGE sulfide deposits (Jinbaoshan, Yingfeng and Zhubu).

5.2. Metal concentrations of 100% sulfides

In order to investigate the origin of the three types of sulfide deposits in the ELIP, we need to know the metal concentrations of pure sulfide melts. To calculate these concentrations, we assume: (1) all of Cu and Ni combined with S to form chalcopyrite ($CuFeS_2$) and pentlandite ($(Fe_{4.5}Ni_{4.5})S_8$, (2) excess S combined with Fe to form pyrrhotite (Fe_9S_8) and pyrite (FeS_2) (Song et al., 2003).

Recalculated to 100% sulfide, the Jinbaoshan PGE ores have the highest PGE contents, the Limahe and Baimazhai Ni–Cu ores have the lowest PGE contents, and the Yangliuping and Qingkuangshan Ni–Cu–PGE ores have

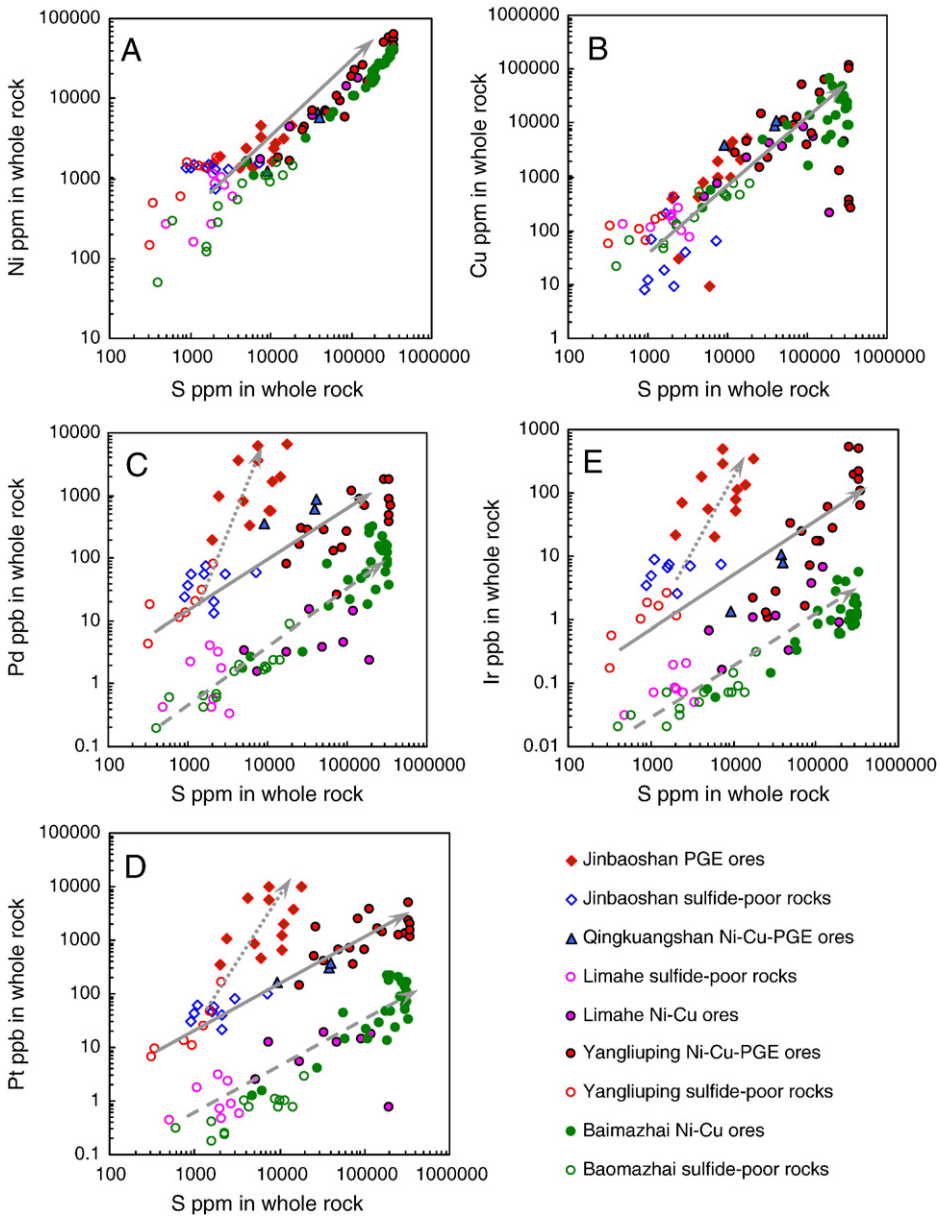

Fig. 3. Plots of Ni, Cu, Pt, Pd, and Ir against S show the distinct trends of the different types of sulfide ores and silicate host rocks.

moderate PGE contents (Fig. 4A–C). The ores in the Jinbaoshan PGE deposit display excellent positive correlations of Pt and Pd versus Ir (Fig. 4B, C) with constant Pd/Ir ratio (~10) (Fig. 4D), whereas Pt and Pd are negatively correlated with Ir for the Ni–Cu and Ni–Cu–PGE sulfide ores with large ranges of Pd/Ir and Pt/Ir ratios. Ruthenium correlates positively with Ir for all three types of deposits (Fig. 4A–C). The Limahe and Baimazhai Ni–Cu sulfide ores have the highest Cu/Pd values, mostly greater than 10^5, whereas Cu/Pd ratios of the Jinbaoshan PGE sulfide ores are lower than 10^4. The Yangliuping and Qingkuangshan Ni–Cu–PGE sulfide ores have Cu/Pd ratios ranging from $>10^5$ to $<10^4$ (Fig. 4E).

5.3. Metal contents of the host intrusions

The metal compositions of the host silicate rocks mimic those of the sulfide ores. The host rocks of the Ni–Cu and Ni–Cu–PGE sulfide deposits have similar ranges of Ni and Cu (18–2200 ppm and 21–750 ppm, respectively), whereas those in the Jinbaoshan sill are rich in Ni and poor in Cu (mostly 700–1500 ppm Ni and less than 70 ppm Cu with the exception of a few samples) (Fig. 3A, B). Particularly, the host rocks in the Jinbaoshan sill contain obviously higher PGE (22–103 ppb Pt, 2–10 ppb Ir) than those of the Ni–Cu sulfide deposits (<3 ppb Pt and 0.3 ppb Ir). The host rocks of the Ni–Cu–PGE sulfide deposits contain 6–50 ppb Pt, and 0.1–2.5 ppb Ir (Table 1, Fig. 3C–E). Positive correlations between Cu, Pt, and Pd with S in the host silicate rocks indicate that there are limited sulfides in the rocks (Table 1, Fig. 3). In addition, the rocks from various intrusions show continuations of trends with the hosted sulfide ores (Fig. 3C–E).

6. Discussions

Magmatic sulfide deposits are formed by sulfide segregation from mantle-derived mafic–ultramafic magmas (e.g. Naldrett, 2004) and their compositions are thus controlled by the compositions of the parental silicate magmas and the processes of sulfide segregation. Because of their extremely high sulfide/silicate liquid partition coefficients (10^3–10^5) (Peach et al., 1990; Stone et al., 1990; Fleet et al., 1991), PGE are highly concentrated in sulfide melts, resulting in depletion of these metals in the residual magmas even after small amounts of sulfide segregation. In contrast, Cu and Ni would be much less depleted in the residual magmas because of their relatively low

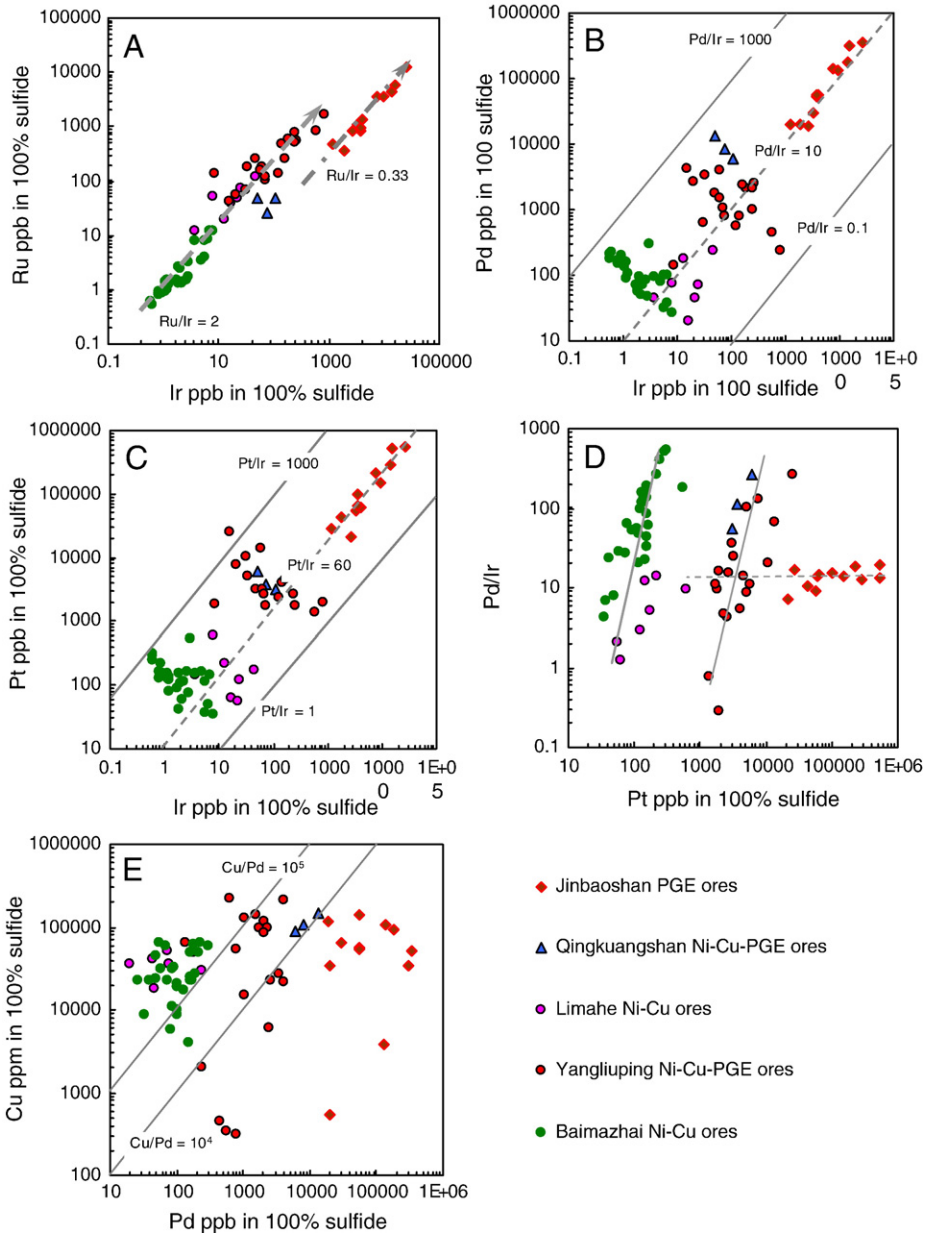

Fig. 4. Compositions of PGE on a 100% sulfide basis. (A–C) Correlations of Ru, Pt, and Pd against Ir; (D) Pd/Ir versus Pt; (E) correlation between Cu and Pd.

sulfide/silicate liquid partition coefficients (10^2–10^3) (Francis, 1990; Peach et al., 1990). Therefore, the original concentrations of Ni, Cu, and PGE in sulfide melts are controlled by both the abundances of these metals in the parental silicate magmas and mass ratios between the silicate magma and sulfide liquid, the *R*-factor (Campbell and Naldrett, 1979). Concentrations of Ni, Cu, and PGE of the sulfide melts may be further modified by reaction with new surges of magma that have variable abundances of these metals (e.g. Naldrett, 2004).

A very important mechanism resulting in compositional variations of sulfide ores is fractionation of sulfide melts. Previous experiments indicate that during fractionation of sulfide melts, Ni, Cu and PPGE (Pd, Pt, and Rh) are incompatible in the early crystal phase, monosulfide solid solution (Mss), and Ir and Ru are compatible (Fleet et al., 1993; Barnes et al., 1997). Consequently, differentiation between IPGE and PPGE is expected during fractional crystallization of sulfide melts (Ebel and Naldrett, 1996; Barnes et al., 1997).

The three types of magmatic sulfide deposits in the ELIP have different Ni, Cu, and PGE contents and distinct correlations between these metals (Figs. 3 and 4). Previous studies of the Yangliuping Ni–Cu–PGE deposits, the Baimazhai Ni–Cu deposit, and the Jinbaoshan PGE deposit were focused on the key factors leading to sulfide segregation (Song et al., 2003, 2006; Wang, 2006; Tao et al., 2007). The mechanisms controlling the grades of PGE and differentiation between these metals were not understood. The discussions below attempt to address the roles of multiple sulfide segregation and diverse fractionation of sulfide liquids on the distinct chemical features and differences among the PGE in the three types of magmatic sulfide deposits.

6.1. Metal concentrations of the parental magmas

Primary mafic magmas derived from partial melting of the upper mantle can be rich in PGE, Ni, and Cu if the molten sulfides are completely dissolved in the magmas (Keays, 1995). Therefore, S-undersaturated primary magmas generally have Cu/Pd ratios similar to that of the mantle, ~7000–10,000 (Barnes and Maier, 1999). Because of the much higher sulfide/silicate liquid partition coefficient for Pd than for Cu, sulfide segregation would result in much more depleted Pd than Cu in the silicate magmas. Thus, Cu/Pd values of sulfide ores obviously higher than

that of the mantle (7000–10,000) indicate an earlier sulfide separation from parental magmas. In contrast, reaction with the PGE undepleted silicate magma would reduce Cu/Pd values of the sulfide melts.

A remarkable characteristic of the Limahe and Baimazhai Ni–Cu sulfide ores is their very high Cu/Pd ratios, mostly higher than 10^5 and up to 10^6, which suggest that the sulfides were separated from strongly PGE-depleted parental magmas that experienced earlier sulfide removal (Fig. 4E). In contrast, low Cu/Pd values of the sparsely disseminated sulfide ores in the Jinbaoshan PGE deposit (27–6300) indicate that the sulfides were segregated from primary PGE-rich mafic magmas and probably reacted with fresh melts (Fig. 4E). The disseminated Ni–Cu–PGE sulfide ores of the Yangliuping and Qingkuangshan deposits have moderate Cu/Pd ratios (5500–90,000), suggesting that the parental silicate magmas were slightly depleted in PGE and experienced previously weak sulfide separation (Fig. 4E).

6.2. Quantitative approaches for sulfide segregation from the silicate magmas

Copper and PPGE are strongly incompatible in silicate minerals and can be concentrated weakly in basaltic magmas during S-undersaturated fractional crystallization. For example, the Siberian basalts containing as high as 13 ppb Pt and Pd did not experience earlier sulfide removal (Brugmann et al., 1993). Previous studies indicate that the S-undersaturated Emeishan continental flood basalts in the northern margin of the ELIP are rich in PGE and contain 10–20 ppb Pd and Pt, 0.1–0.2 ppb Ir, 0.1–0.3 ppb Ru, 0.3–0.6 ppb Rh, and 100–250 ppm Cu (Song et al., 2006).

Metal contents of sulfide melts and their relationship with the *R*-factor can be illustrated using the equation of Campbell and Naldrett (1979)

$$C_l^{sul} = C_l^{sil} * D_i * (R+1)/(R+D_i) \quad (1)$$

Where C_i^{sul} and C_i^{sil} represent the concentrations of element *i* in the sulfide melt and in the parental silicate magma, respectively, D_i is the sulfide melt/silicate liquid partition coefficient of element *i*, and *R* is the *R*-factor. Thus, the concentrations of chalcophile elements in sulfide liquids are a function of their abundances in parental silicate magmas, sulfide melt/silicate liquid partition coefficients, and the *R*-factor.

We assume that the ELIP basaltic magmas had 15 ppb Pt, 22 ppb Pd, 1 ppb Ir, and 200 ppm Cu before reaching S-saturation. Nickel abundances in the parental magmas are difficult to predict because of possible fractional crystallization of olivine. High-Mg continental tholeiites and ocean island basalts contain 100–200 ppm Ni (Davis and Tredoux, 1985; Von Gruenewaldt et al., 1989; Barnes and Picard, 1993; Fryer and Greenough, 1995). We assume that the Ni abundance in basaltic magmas before sulfide segregation is about 200 ppm. Platinum and Pd have sulfide/silicate liquid partition coefficients of about 20,000, and Ni and Cu have coefficients of 500 and 1000, respectively (Fleet et al., 1991; Francis, 1990). These coefficients are assumed to be constant during sulfide segregation, although partitioning of chalcophile and siderophile elements between sulfide and silicate liquids may change slightly depending on temperature, concentrations of these metals in the sulfide melt, and MgO content in the parental magma (Naldrett, 2004).

Our model calculations according to Eq. (1) indicate that Pd in sulfide liquids increases markedly as *R*-factors increase from 10^3 to 10^5, whereas Ni contents remain nearly constant if the *R*-factor is larger then change little until the *R* values are less than 1000 (Fig. 5). To avoid the notable effect of fractionation of sulfide liquids, only disseminated sulfide ores (in 100% sulfide basis) from the three types of deposits are plotted in Fig. 5. When the assumed basaltic magma reached S-saturation, the segregated sulfide liquids would contain 21–370 ppm Pd and 6.7×10^4–10^5 ppm Ni (under $R=10^3$–10^5), which are roughly consistent with the contents of Pd and Ni of the pure sulfide melts of the Jinbaoshan PGE ores (21–545 ppm and >55,200 ppm, respectively) assuming that *R* values varied from 10^3 to 10^5 (Fig. 5). The very high *R*-factors are consistent with the extremely low volume percentages of sulfides in the Jinbaoshan PGE ores.

The Pd contents in the pure sulfide melts of the disseminated Ni–Cu–PGE ores in the Yangliuping and Qingkuangshan deposits are lower than the calculated PGE-rich values even at *R*-factors as low as 100, suggesting that their parental magmas were PGE-depleted because of earlier sulfide removal. This is consistent with the high Cu/Pd ratios of the disseminated Ni–Cu–PGE ores (5500–90,000, higher than that of the mantle ~7000–10,000) (Fig. 4E). If about 0.01% sulfide melt was removed from the PGE-rich magma, the residual magma would contain 2 ppb Pt, 3 ppb Pd, and 190 ppm Ni according to Rayleigh's law ($C_i^L/C_i^O = F^{(D_i-1)}$, in which C_i^O and C_i^L represent abundances of element *i* in the original and residual magmas, respectively). The contents of Pd in the sulfide melts that segregated from such a PGE-weakly depleted magma would evidently be lower than those from a PGE-rich magma and can match the pure sulfide melts of the disseminated ores in the Yangliuping and Qingkuangshan Ni–Cu–PGE deposits if the *R*-factors range from 5000 to <1000 (Fig. 5).

The extremely high Cu/Pd ratios (>10^5) of the PGE-poor sulfides in the Baimazhai and Limahe Ni–Cu deposits suggest that their parental magmas were strongly depleted in PGE. Calculations according to Rayleigh's law indicate that 0.025% sulfide melt removal from the PGE-rich parental magma would give rise to a the residual magma contained only 0.1 ppb Pt, 0.15 ppb Pd, and 177 ppm Ni. The calculated correlation between Pd and Ni of the sulfide liquids that segregated from such strongly PGE-depleted magma matches well plots of the pure sulfides of the disseminated ores in the Baimazhai and Limahe Ni–Cu deposits if the *R*-factors range from 300 to 2000 (Fig. 5). The *R*-factors are much higher than that given by Wang (2006) for the massive sulfides in the Baimazhai Ni–Cu deposit ($R=70$), probably because their calculation did not consider the effect of prior sulfide removal on the concentrations of chalcophile elements in the silicate magma.

The above model calculations indicate that the sulfide melts of the three types of deposits were segregated from different parental silicate magmas having variable PGE abundances. Multiple sulfide segregation played a very important role for the low PGE concentrations of the Limahe and Baimazhai Ni–Cu sulfide deposits.

6.3. Effects of fractionation of sulfide melts

Because all PGE are typically partitioned in the sulfide liquid when immiscibility occurs, neither sulfide liquid segregation nor reaction with fresh magma cause significant differentiation of these metals. The remarkably negative correlations of Pt and Pd against Ir in the Ni–Cu–PGE and Ni–Cu sulfide ores (Fig. 4B–D) suggest that fractionation of sulfide melts has played roles on the compositional variations of the sulfide ores. However, the relatively constant Pd/Ir ratios (from 7 to 20) of the Jinbaoshan PGE-rich sulfide ores indicate that their compositions were not modified by fractionation of sulfide melts (Fig. 6). The low Pd/Ir ratios of the Jinbaoshan sulfides indicate earlier removal of IPGE by chromite and olivine before S-saturation. If the primary basaltic magma contained 200 ppm Ni, 22 ppb Pd, and 1 ppb Ir, as assumed above, sulfides segregated under *R* values ranging from 10^3 to 10^6 would have Ni/Ir ratios ranging from 6000 to 70,000, comparable with those of the Jinbaoshan sulfides (Ni/Ir=7265 to 74,238), and Pd/Ir ratios (~22), slightly higher than those of the Jinbaoshan sulfides (Pd/Ir=7–20) (Fig. 6).

Experimental studies indicate that the first phase to crystallize from a sulfide melt is Mss at temperatures above 1100 °C (Kullerud et al., 1969; Naldrett et al., 1967; Misra and Flet, 1973, 1974). The Mss/sulfide liquid partition coefficients (D_i) of Ir, Ru, and Rh are 3.4–11, 4.2, and 1–3, respectively and those of Pt, Pd, Cu, and Ni are 0.05–0.2, 0.09–0.2, 0.2–0.3, and 0.36–0.84, respectively (Fleet et al., 1993; Barnes et al., 1997). Recent experimental studies indicate that D_{Pt} and D_{Pd} increase slightly with decreasing temperature, but Pt and Pd and Cu remain incompatible

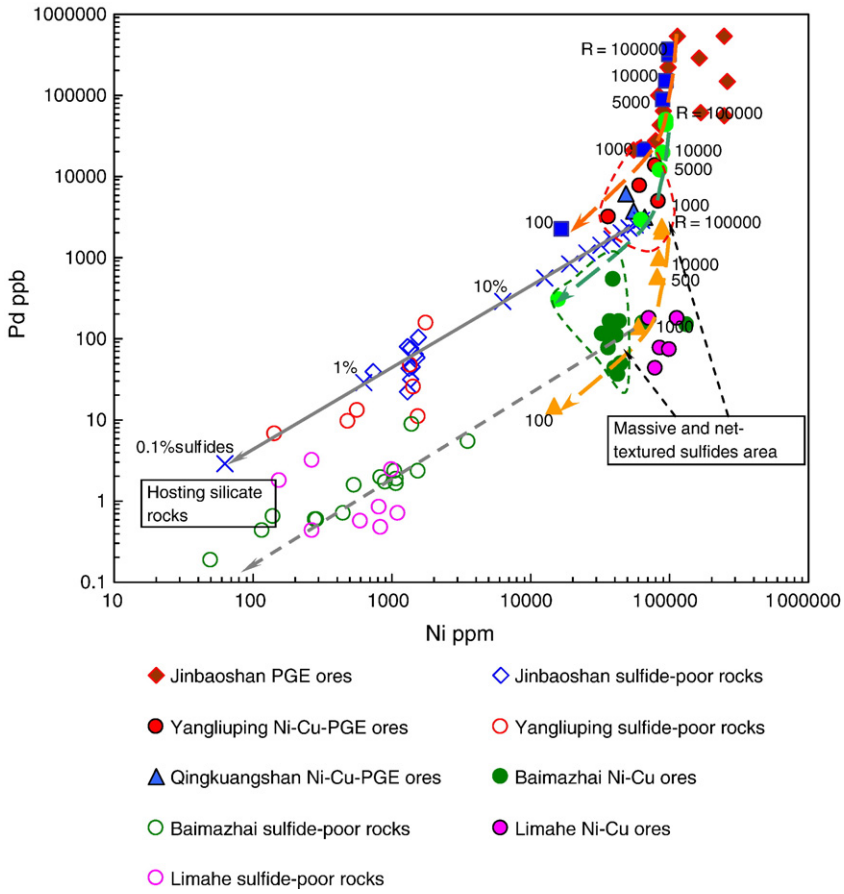

Fig. 5. Model calculation of the variation of Pd with Ni in the disseminated ores of the three types of deposits and the silicate host rocks. The Pd and Ni concentrations of the disseminated sulfides are on a 100% sulfide basis, whereas the Pd and Ni concentrations of the silicate rocks are on a whole-rock basis, showing that they contain small amounts of sulfides. Blue solid squares present the sulfide melts segregated from PGE-rich basaltic magma with 15 ppb Pt, 22 ppb Pd, and 200 ppm Ni under variable *R* values (labeled in the diagram). Green solid points display sulfide liquids separated from PGE-weakly depleted magma with 2 ppb Pt, 3 ppb Pd, and 190 ppm Ni (because of 0.001% sulfide removal from PGE-rich magma) under different *R* values. Yellow triangles show the sulfide liquids produced by sulfide immiscibility in the PGE-heavily depleted magma with 0.1 ppb Pt, 0.15 ppb Pd, and 177 ppm Ni (because of 0.025% sulfide removal from PGE-rich magma). Concentrations of Pd and Ni in the sulfide barren rocks increase when they contain small amount of sulfides as shown by the grey lines. Percentages of sulfide in the sulfide-poor rocks are labeled as *n*%.

with Mss under the range of temperature, f_{O_2} and f_{S_2}, of natural sulfide melts (Barnes et al., 2001; Ballhaus et al., 2001; Fleet et al., 1993, 1999a, b). At low f_{O_2} and f_{S_2}, Ir and Rh would become incompatible for Mss, whereas Ru is strongly compatible with Mss under all conditions, with D_{Ru} ranging from a maximum of 14.5 to a minimum of 1.8 (Mungall et al., 2005). D_{Ni} is as low as 0.23 at low f_{O_2} and f_{S_2} and shows a moderate increase as f_{S_2} increases and temperature decreases to reach a maximum of 0.9 at 950 °C (e.g. Barnes et al., 1997). Mungall et al. (2005) estimated that Ni would become compatible with Mss at f_{O_2} slightly higher than QFM and temperature slightly lower than 950 °C.

Negative correlations between Ir vs Pt and Pd for the sulfides of the Ni–Cu–PGE and Ni–Cu deposits (Fig. 4B and C) indicate that Ir was compatible during fractionation of Mss in these rocks. Thus, the sulfide melts of these two types of deposits became enriched in Ni, Cu, Pt and Pd relative to Ir, Ru, and Rh, and thus had higher Pd/Ir and Ni/Ir ratios during fractionation of Mss.

There are two extreme models describing magmatic fractionation: fractional crystallization and equilibrium crystallization. In Fig. 6, we compare the results of numerical models of fractional and equilibrium crystallization of Mss with the data sets from the sulfide ores of the Yangliuping and Qingkuangshan Ni–Cu–PGE deposits and the Limahe and Baimazhai Ni–Cu deposits. An outstanding feature of the data as illustrated in Fig. 6 is that the Ni–Cu–PGE and Ni–Cu sulfides plot along separate trends. Some samples show considerable scatter of Ni/Ir values, which could be the result of either late magmatic or deuteric alteration, or alternatively the result of subsequent metamorphism. In the calculations used in this study, we assume D_{Pt}, D_{Pd}, D_{Ir}, and D_{Cu} between Mss and sulfide melt to be 0.14, 0.13, 10, 0.22, respectively and that they remained constant during fractionation (Fleet et al., 1993; Barnes et al., 1997). We further assume that D_{Ni} begins at 0.5 and increases to 0.9 when >50% of the system has solidified under decreasing temperature (Mungall et al., 2005). The fractionating phase is taken to be Mss.

6.3.1. Fractional crystallization of Mss for Ni–Cu–PGE sulfides

According to the calculation of sulfide segregation shown in Fig. 5, sulfide melts from which the Ni–Cu–PGE deposits formed separated from a weakly PGE-depleted parental magma containing 3 ppb Pd, 0.14 ppb Ir, and 190 ppm Ni under an *R*-factor of 1000 would contain 2841 ppb Pd, 129 ppb Ir, and 63,397 ppm Ni. Fractional crystallization of Mss up to 25% will result in changes in the Pd/Ir and Ni/Ir ratios of such a sulfide melt from 22 to 377, and from 4.9×10^5 to 7.0×10^6, respectively (Fig. 6, Model 1 liquids). In contrast, equilibrium crystallization of Mss leads to slow differentiation of sulfide liquids. According to our model calculation, Pd/Ir and Ni/Ir ratios of the sulfide melt would be elevated to 3.1×10^6 and 411, respectively, after 70% equilibrium crystallization of Mss (Fig. 6 Model 2 liquids). The Mss cumulates produced by both fractional and equilibrium crystallization have Pd/Ir and Ni/Ir ratios lower than the initial values of the original sulfide melts (Fig. 6, Model 1 cumulates and Model 2 cumulates, respectively).

In the Yangliuping area, the sulfides gravitationally settled into the lower parts of the mafic–ultramafic sills and the remaining PGE-depleted magmas erupted to form the flood basalts (Fig. 2A) (Song et al.,

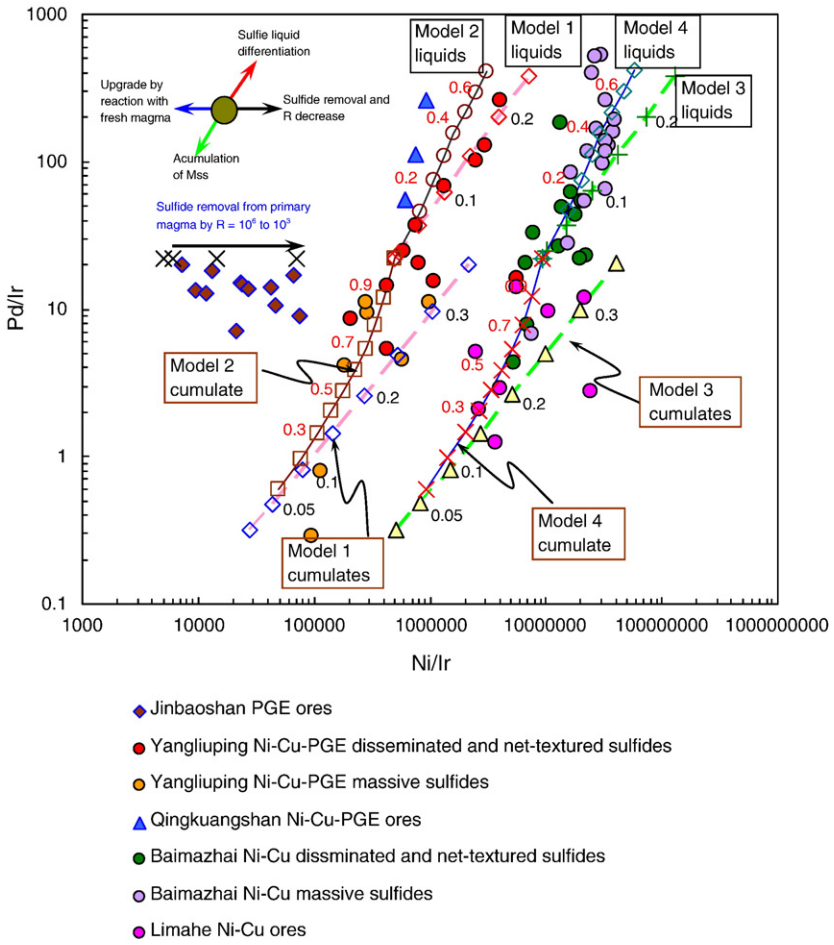

Fig. 6. Model calculations for fractional and equilibrium crystallization of Mss from sulfide liquids similar to the three types of magmatic sulfide deposits in the ELIP. Liquid and cumulate trends are calculated using the Rayleigh equation or equilibrium crystallization equation (ticks with numbers, like 0.2, indicate degree of fractionation). Models 1 and 2 present the trends of fractional and equilibrium crystallization of the Ni–Cu–PGE sulfides, respectively. Models 3 and 4 display the trends of fractional and equilibrium crystallization of the Ni–Cu sulfides, respectively. Pd/Ir and Ni/Ir ratios of the Yangliuping disseminated and net-textured sulfides are consistent with Model 1 liquids, whereas these ratios in the massive sulfides roughly match those of Model 1 and 2 cumulates, suggesting that the differentiation of the Yangliuping sulfides was controlled dominantly by fractional crystallization of Mss. In contrast, the Baimazhai sulfides mainly plot on the trend of Model 2 liquids, indicating that equilibrium crystallization of Mss played an important role for the sulfide liquid fractionation.

2003, 2004, 2006). Gravity settling of the sulfide melt formed a sulfide zone at the bottom and an overlying silicate crystal mush zone with interstitial. The Yangliuping disseminated and net-textured sulfides plot on the liquid trend of fractional crystallization of Mss (Model 1 liquids) with high Pd/Ir and Ni/Ir ratios, whereas the massive sulfides plot around the Model 1 and Model 2 cumulates (Fig. 6). The high Pd/Ir and Ni/Ir values of the disseminated and net-textured sulfides can be explained by about 20% fractional crystallization of Mss. However, it is very difficult to separate the crystallized Mss from the sulfide liquid and to prevent them from reacting completely. The low Pd/Ir and Ni/Ir ratios of the massive sulfide can be accounted for as a mixture between sulfide liquids and Mss and reaction with interstitial sulfide melts (Fig. 6). The calculation indicates that the compositional variations of the Yangliuping sulfides were dominated mainly by fractional crystallization of Mss.

In the Qingkuangshan dike-like ultramafic intrusion, sulfides are concentrated in the middle of the intrusion, which may be the root of a large mafic–ultramafic intrusion or a magma conduit. High Pd/Ir ratios of the Qingkuangshan Ni–Cu–PGE sulfides indicate fractionation of Mss, whereas low Ni/Ir ratios (even lower than the Model 2 liquids) of the ores may reflect parental magma compositions having low Ni/Ir ratios and/or reaction of sulfides with fresh magma (Fig. 6).

6.3.2. Equilibrium crystallization of Mss in the Ni–Cu deposits

The Ni–Cu sulfides that separated from strongly PGE-depleted silicate magma containing 0.15 ppb Pd, 0.007 ppb Ir, and 177 ppm Ni under an *R*-factor of 1000 would contain 143 ppb Pd, 6.4 ppb Ir, and 59,059 ppm Ni. Twenty-five percent fractional crystallization of Mss would cause the Pd/Ir ratio of such sulfide melt to change from 22 to 381 and the Ni/Ir ratio from 9.2×10^6 to 1.3×10^8 (Fig. 6, Model 3 liquids). On the other hand, up to 70% equilibrium crystallization of Mss would increase the Pd/Ir and Ni/Ir ratios of the residual sulfide melts to 416 and 5.7×10^7, respectively (Fig. 6, Model 4 liquids). As shown in Fig. 6, most of the Baimazhai Ni–Cu sulfides plot on the trend of equilibrium crystallization of Mss (Model 4 liquids), suggesting that their compositional variations were controlled by this process. In addition, the high Pd/Ir and Ni/Ir ratios indicate that the massive sulfides reflect more extensive fractionation of Mss (~70%) compared to the disseminated and net-textured sulfides (Fig. 6).

We propose that sulfide segregation occurred in a staging magma chamber at depth. Sulfide melt separated from silicate magma and segregated to the bottom of the staging chamber to form a sulfide melt zone. Compared to the interstitial sulfides between the silicates, the sulfide melts at the bottom of the staging chamber experienced more extensive crystallization of Mss. The crystallized Mss more or less continuously reacted with the sulfide liquid. The differentiated sulfide melts at the top of the sulfide melt zone have high Pd/Ir and Ni/Ir ratios. Thus, the Baimazhai sulfides mostly plot on the trend of equilibrium crystallization of Mss (Model 4 liquid). The staging chamber was subsequently evacuated from its top downward due to regional compressive forces. The extensively differentiated sulfide

magma from the bottom of the staging chamber intruded latest and formed massive sulfides with high Pd/Ir and Ni/Ir ratios at the core of the Baimazhai intrusion. Correspondingly, the massive ore body has sharp contacts with the silicate units of the intrusion and locally intrudes the wall rocks. The sharp boundaries of the massive sulfides are original and do not related to late faults.

In contrast, the Limahe Ni–Cu sulfides plot between the cumulate trends of fractional and equilibrium crystallization of Mss (Fig. 6, Model 3 and 4 cumulates). The low Pd/Ir and Ni/Ir values of the Limahe sulfides probably suggest that fractionated sulfide melts had been squeezed out.

6.4. Significance of the host silicate rock compositions

When sulfur saturation is achieved, sulfides will start to separate gradually from the silicate magma. There are always minor sulfides remaining in the residual magma, in which PGE are positively correlated with S, Ni and Cu. In diagrams of PGE versus S (Fig. 3), the silicate host rocks overlap with the sulfide ores and show positive correlations between PGE and S, indicating that the silicate rocks formed by solidification of the residual magmas with minor relict sulfides. A very important point is that the silicate rocks hosting the various types of sulfide deposits plot on distinct trends in Fig. 3. The rocks in the Jinbaoshan sill are richest in PGE, corresponding to the highest PGE contents in the sulfide ores. In contrast, the silicate host rocks of the Limahe and Baimazhai Ni–Cu deposits are the lowest in PGE (Fig. 3C–E) and contain small amounts of the sulfide melt (<3%) separated from the highly PGE-depleted magma under an *R*-factor ~1000 as shown in Fig. 5. The silicate rocks hosting the Ni–Cu–PGE deposits have moderate PGE concentrations (Fig. 3C–E) and generally contain less than 3% sulfides (Fig. 5). Therefore, the PGE concentrations of the hosting silicate rocks can be used to predict what type of magmatic sulfide mineralization has occurred.

7. Conclusions

The most important controlling factors on Ni, Cu, and PGE contents of magmatic sulfides include (1) abundances of the metals in the parental magmas, (2) amounts of sulfide liquid separated, (3) fractionation of the sulfide melts, and (4) reaction with new surges of magma.

The three types of magmatic sulfide deposits in the ELIP, including PGE, Ni–Cu–PGE, and Ni–Cu deposits, are distinguished by PGE contents in the sulfide ores and were produced by different processes as shown by Fig. 7. The Jinbaoshan Pt–Pd deposit contains only minor sulfides that were produced by very weak sulfide segregation from PGE-rich parental magmas. The sulfides of the Ni–Cu–PGE deposits (e.g. Yangliuping and Qingkuangshan) and Ni–Cu deposits (e.g. Limahe and Baimazhai) were produced by extensive sulfide segregation from weakly and strongly PGE-depleted magmas, respectively because of earlier sulfide removal. Model calculations indicate that the sulfide melts in the Ni–Cu–PGE deposits and Ni–Cu deposits were overprinted by fractional and equilibrium crystallization of Mss, respectively. The silicate host rocks of the different types of magmatic sulfide deposits have distinct PGE abundances, which can be used to predict the type of associated magmatic sulfide deposit.

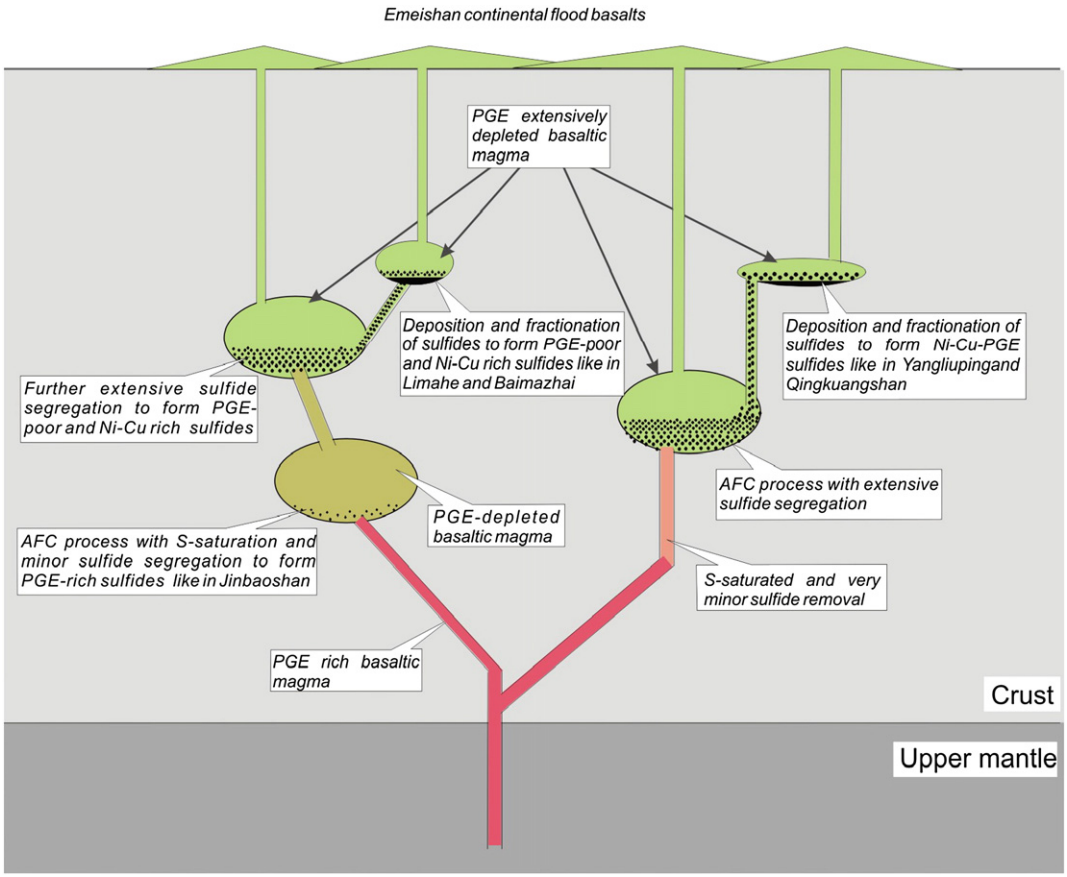

Fig. 7. A petrogenetic model showing the formation of the three types of magmatic sulfide deposits in the ELIP. The Pt–Pd deposits containing minor sulfides, like the Jinbaoshan deposit, were formed by very weak sulfide segregation from PGE-rich parental magmas. The Ni–Cu–PGE deposits (e.g. Yangliuping and Qingkuangshan) were related to extensive sulfide segregation from weakly PGE-depleted basaltic magmas because of prior sulfide separation. On the other hand, the Ni–Cu deposits (e.g. Limahe and Baimazhai) were produced by extensive sulfide segregation from strongly PGE-depleted magmas because of earlier sulfide removals.

Acknowledgements

This study was supported by 973 Program (2007CB411408) and research grants from NSFC (40573014, 40730420) and "CAS Hundred Talents" Project from Chinese Academy of Sciences to X.-Y. Song and Research Grant Council of Hong Kong SAR (China) (HKU7057/05P) to M.-F. Zhou. We are very grateful to Dr. L. Qi and Ms. X. Fu for their kind help with the lab work. We thank Professor Tony Naldrett for his thorough reviews and Professor D. Rickard for handling this paper.

References

Ballhaus, C., Tredoux, M., Spath, A., 2001. Phase relations in the Fe–Ni–Cu–PGE–S system at magmatic temperature and application to the massive sulphide ores of the Sudbury Igneous Complex. J. Petrol. 42, 1911–1926.

Barnes, S.J., Picard, C.P., 1993. The behavior of platinum-group elements during partial melting, crystal fractionation and sulphide segregation: an example from the Cap Smith fold belt, northern Quebec. Geochim. Cosmochim. Acta 57, 79–87.

Barnes, S.-J., Maier, W.D., 1999. The fractionation of Ni, Cu and the noble metals in silicate and sulfide liquids. In: Keays, R.R., Lesher, C.M., Lightfoot, P.C., Farrow, C.E.G. (Eds.), Dynamic Processes in Magmatic Ore Deposits and their Application in Mineral Exploration. Geol. Assoc. Canada Short Course, vol. 13, pp. 69–106.

Barnes, S.-J., Makovicky, E., Karup-Moller, S., Makovicky, M., Rose-Hansen, J., 1997. Partition coefficients for Ni, Cu, Pd, Pt, Rh and Ir between monosulfide solid solution and sulfide liquid and the implication for the formation of compositionally zoned Ni–Cu sulfide bodies by fractional crystallization of sulfide liquid. Can. J. Earth Sci. 34, 366–374.

Barnes, S.-J., van Achterbergh, H., Makovicky, E., Li, C., 2001. Proton microprobe results for the partitioning of platinum-group elements between monosulfide solid solution and sulphide liquid. S. Afr. J. Geol. 104, 275–286.

Brozdowki, R.A., Page, M.L., 2004. Jinbaoshan (JBS) Pt–Pd–Ni–Cu deposit, Yunnan, P. R. China. In: Shellnutt, J.G., Zhou, M.F., Pang, K.N. (Eds.), Recent Advances in Magmatic Ore Systems in Mafic–Ultramafic Rocks, Abstract vol. of IGCP 479 Hong Kong Workshop, pp. 67–69.

Brugmann, G.E., Naldrett, A.J., Asif, M., Lightfoot, P.C., Gorbachev, N.S., Fedorenko, V.A., 1993. Siderophile and chalcophile metals as traces of the evolution of the Siberian Traps in the Noril'sk region, Russia. Geochim. Cosmochim. Acta, 57, 2001–2018.

Burchfiel, B.C., Chen, Z., Liu, Y., Royden, L.H., 1995. Tectonics of the Longmen Shan and adjacent regions, central China. Int. Geol. Rev. 37, 661–735.

Campbell, I.H., Naldrett, A.J., 1979. The influence of silicate:sulfide ratios on the geochemistry of magmatic sulfides. Econ. Geol. 74, 1503–1506.

Chai, G., Naldrett, A.J., 1992. Characteristics of Ni–Cu–PGE mineralisation and genesis of the Jinchuan deposit, Northwest China. Econ. Geol. 87, 1475–1495.

Chung, S.L., Jahn, B.M., 1995. Plume–lithosphere interaction in generation of the Emeishan flood basalts at the Permian–Triassic boundary. Geology 23, 889–892.

Davis, G., Tredoux, M., 1985. The platinum-group element and gold contents of the marginal rocks and sills of the Bushveld complex. Econ. Geol. 80, 838–848.

Ebel, D.S., Naldrett, A.J., 1996. Fractional crystallization of sulfide ore liquids at high temperature. Econ. Geol. 91, 607–637.

Fleet, M.E., Stone, W.E., Crocket, J.H., 1991. Partitioning of palladium, iridium, platinum, between sulfide liquid and basaltic melt: effects of melt composition, concentration, and oxygen fugacity. Geochim. Cosmochim. Acta 55, 2545–2554.

Fleet, M.E., Chryssoulis, S.L., Stone, W.E., Weisener, C.G., 1993. Partition of platinum-group elements and Au in the Fe–Ni–Cu–S system: experiments on the fractional crystallization of sulfide melt. Contrib. Mineral. Petrol. 115, 36–44.

Fleet, M.E., Crocket, J.H., Liu, M., Stone, W.E., 1999a. Laboratory partitioning of platinum-group elements (PGE) and gold with application to magmatic sulfide–PGE deposits. Lithos 47, 127–142.

Fleet, M.E., Liu, M., Crocket, J.H., 1999b. Partitioning of trace amounts of highly siderophile elements in the Fe–Ni–S system and their fractionation in nature. Geochim. Cosmochim. Acta. 63, 2611–2622.

Francis, R.D., 1990. Sulfide globules in mid-ocean ridge basalts (MORB) and the effect of oxygen abundance in Fe–S–O liquids on the ability of those liquids to partition metals from MORB and komatiitic magmas. Chem. Geol. 85, 199–213.

Fryer, B.J., Greenough, J.D., 1995. Evidence for mantle heterogeneity from platinum-group element abundances in Indian Ocean basalts. Can. J. Earth Sci. 29, 2329–2339.

Glotov, A.I., Polyakov, G.V., Hoa, T.T., Balykin, P.A., Akimtsev, V.A., Krivenko, A.P., Tolstykh, N.D., Phuong, N.T., Thanh, H.H., Hung, T.Q., Petrova, T.E., 2001. The Ban Phuc Ni–Cu–PGE deposit related to the Phanerozoic komatiite-basalt association in the Song Da Rift, northwestern Vietnam. Can. Mineral. 39, 573–589.

Keays, R.R., 1995. The role of komatiitic and picritic magmatism and S-saturation in the formation of ore deposits. Lithos 34, 1–18.

Kullerud, G., Yund, R.A., Moh, G.H., 1969. Phase relations in the Cu–Fe–S, Cu–Ni–S and Fe–Ni–S systems. Econ. Geol. 4, 323–343.

Misra, K.C., Flet, M.E., 1973. The chemical composition of synthetic and natural pentlandite assemblages. Econ. Geol. 68, 518–539.

Misra, K.C., Flet, M.E., 1974. Chemical composition and stability of violarite. Econ. Geol. 69, 391–403.

Mungall, J.E., Andrews, D.R.A., Cabri, L.J., Sylvester, P.J., Tubrett, M., 2005. Partitioning of Cu, Ni, Au, and platinum-group elements between monosulfide solid solution and sulfide melt under controlled oxygen and sulfur fugacities. Geochim. Cosmochim. Acta. 69, 4349–4360.

Li, C., Maier, W.D., de Waal, S.A., 2001. Magmatic Ni–Cu versus PGE deposits: contrasting genetic controls and exploration implications. South African J. Geol. 104, 309–318.

Naldrett, A.J., 2004. Magmatic Sulfide Deposits: Geology, Geochemistry and Exploration. Springer, New York, p. 727.

Naldrett, A.J., Craig, J.R., Kullerud, G., 1967. The central potion of the Fe–Ni–S system and its bearing on pentlandite solution in iron–nickel sulfide ores. Econ. Geol. 62, 826–847.

Naldrett, A.J., Fedorenko, V.A., Lightfoot, P.C., Gorbachev, N.S., Doherty, W., Asif, M., Lin, S., Johan, Z., 1995. A model for the formation of the Ni–Cu–PGE deposits of the Noril'sk. Trans. Inst. Mining Metal. 104, B18–B36.

Naldrett, A.J., Asif, M., Krstic, S., Li, C., 2000. The composition of mineralization at the Voisey's Bay Ni–Cu sulfide deposit, with special reference to platinum-group elements. Econ. Geol. 95, 845–865.

Peach, C.L., Mathez, E.A., Keays, R.R., 1990. Sulfide melt–silicate melt distribution coefficients for noble metals and other chalcophile elements as deduced from MORB: implication for partial melting. Geochim. Cosmochim. Acta 54, 3379–3389.

Qi, L., Zhou, M.F., Wang, C.Y., 2004. Determination of low concentrations of platinum group elements in geological samples by ID-ICP-MS. J. Anal. Atomic Spect. 19, 1335–1339.

Song, X.-Y., Zhou, M.-F., Hou, Z.-Q., Cao, Z.-M., Wang, Y.-L., Li, Y.-G., 2001. Geochemical constrains on the mantle source of the Upper Permian Emeishan Continental Flood Basalts, Southwestern China. Int. Geol. Rev. 43, 213–225.

Song, X.-Y., Zhou, M.-F., Cao, Z.-M., Sun, M., Wang, Y.-L., 2003. The Ni–Cu–(PGE) magmatic sulfide deposits in the Yangliuping area within the Permian Emeishan large igneous province, SW China. Mineral. Deposita. 38, 831–843.

Song, X.-Y., Zhou, M.-F., Cao, Z.-M., 2004. Genetic relationships between base-metal sulfides and platinum-group minerals in the Yangliuping Ni–Cu–(PGE) sulfide deposit, SW China. Can. Mineral. 42, 469–484.

Song, X.-Y., Zhong, H., Zhou, M.-F., Tao, Y., 2005. Magmatic sulfide deposits in the Permian Emeishan Large Igneous Province, SW China. In: Mao, J.W., Bierlein, F.P. (Eds.), Mineral Deposit Research: Meeting the Global Challenge (the 8th Biennial SGA Meeting in Beijing), 1. Springer, Berlin, pp. 465–468. ISBN-10.

Song, X.-Y., Zhou, M.-F., Keays, R.R., Cao, Z.-M., Sun, M., Qi, L., 2006. Geochemistry of the Emeishan flood basalts at Yangliuping, Sichuan, SW China: implication for sulfide segregation. Contrib. Mineral. Petrol. 152, 53–74.

Stone, W.E., Crocket, J.H., Fleet, M.E., 1990. Partitioning of palladium, iridium, platinum, and gold between sulfide liquid and basaltic melt at 1200 C. Geochim. Cosmochim. Acta 54, 2341–2344.

Tao, Y., Li, C., Hu, R.-Z., Ripley, E.M., Du, A.-D., Zhong, H., 2007. Petrogenesis of the Pt–Pd mineralized Jinbaoshan ultramafic intrusion in the Permian Emeishan Large Igneous Province, SW China. Contrib. Mineral. Petrol. 153, 321–337.

Tao, Y., Li, C., Song, X.-Y., Ripley, E.M., submitted for publication. Mineralogical, petrological and geochemical studies of the Limahe mafic-ultramatic intrusion and the associated Ni-Cu sulfide ores. Miner. Depos.

Von Gruenewaldt, G., Hulbert, L.J., Naldrett, A.J., 1989. Constraining platinum-group element concentration patterns in cumulates of the Bushveld Complex. Mineral. Deposita. 24, 219–229.

Wang, Y., 2006. Petrogenesis of Permian flood basalts and mafic–ultramafic intrusions in the Jinping (SW China) and Song Da (Northern Vietnam) districts. PhD thesis of The University of Hong Kong.

Wang, C.Y., Zhou, M.-F., 2006. Geochemical constraints on the origin of the Permian Baimazhai mafic–ultramafic intrusion, SW China. Contrib. Mineral. Petrol. 152, 309–321.

Xu, Y.-G., Chung, S.L., Jahn, B.M., Wu, G.-Y., 2001. Petrologic and geochemical constraints on the petrogenesis of Permian–Triassic Emeishan flood basalts in southwestern China. Lithos 58, 145–168.

Xu, Y.G., He, B., Chung, S.-L., Menzies, M.A., Frey, F.A., 2004. Geologic, geochemical, and geophysical consequences of plume involvement in the Emeishan flood-basalt province. Geology 32, 917–920.

Yang, Y.-T., 1989. Research Report of the Jinbaoshan Pt–Pd deposit, Midu County, Yunnan Province (in Chinese). Geological Bureau of Yunnan Province.

Yao, J.-D., 1988. Genesis of Magmatic Cu–(Pt)–Ni Sulfide Deposit in the Xichuan Region (in Chinese). Chongqing Publishing House, Chongqing, China.

Zhang, X.Y., Luo, Y.N., 1988. Panxi Rift. Geological Publishing House (in Chinese), Beijing, China.

Zhong, H., Zhou, X.H., Zhou, M.F., Sun, M., Liu, B.G., 2002. Platinum-group element geochemistry of the Hongge Fe–V–Ti deposit in the Pan-Xi area, southwestern China. Mineral. Depos. 37, 226–239.

Zhong, H., Yao, Y., Hu, S.F., 2003. Trace-element and Sr–Nd isotopic geochemistry of the PGE-bearing Hongge layered intrusion, southwestern China. Int. Geol. Rev. 45, 371–382.

Zhong, H., Yao, Y., Prevec, S.A., Wilson, A.H., Viljoen, M.J., Viljoen, R.P., Liu, B.G., Luo, Y.N., 2004. Trace-element and Sr–Nd isotopic geochemistry of the PGE-bearing Xinjie layered intrusion in SW China. Chem. Geol. 203, 237–252.

Zhou, M.-F., 2004. Geochemical constraints on the diversity of igneous assemblages within the Permian Emeishan large igneous province, SW China. In: Shellnutt, J.G., Zhou, M.-F., Pang, K.N. (Eds.), Recent Advances in Magmatic Ore Systems in Mafic–Ultramafic Rocks, Abstract vol. of IGCP 479 Hong Kong Workshop, pp. 61–63.

Zhou, M.-F., Yang, Z.-X., Song, X.-Y., Keays, R.R., Lesher, C.M., 2002a. Magmatic Ni–Cu–(PGE) sulfide deposits in China. In: Cabri, L.J. (Ed.), The Geology, Geochemistry, Mineralogy, Mineral Benification of the PGE. Can. Inst. Min., Metal. Petrol., Spec., vol 54, pp. 619–636.

Zhou, M.-F., Malpas, J., Song, X.-Y., Robinson, P.T., Sun, M., Kennedy, A.K., Lesher, C.M., Keays, R.R., 2002b. A temporal link between the Emeishan Large Igneous Province (SW China) and the end-Guadalupian mass extinction. Earth Planet Sci. Lett. 196, 113–122.

Zhou, M.-F., Robinson, P.T., Lesher, C.M., Keays, R.R., Zhang, C.J., Malpas, J., 2005. Geochemistry, petrogenesis, and metallogenesis of the Panzhihua gabbroic layered intrusion and associated Fe–Ti– V-oxide deposits, Sichuan Province, SW China. J. Petrol vol. 46, 2253–2280.